





Cite this: *RSC Adv.*, 2022, 12, 17020

# Coumarin derivatives inhibit the aggregation of $\beta$ -lactoglobulin †

Hasan Parvej, <sup>a</sup> Shahnaz Begum,<sup>a</sup> Ramkrishna Dalui,<sup>a</sup> Swarnali Paul,<sup>a</sup> Barun Mondal,<sup>a</sup> Subrata Sardar,<sup>a</sup> Nayim Sepay, <sup>b</sup> Gourhari Maiti<sup>a</sup> and Umesh Chandra Halder <sup>\*a</sup>

The binding of a small molecule to a protein through non-covalent interactions mainly depends on its size and electronic environment. Such binding can change the stability of the three dimensional protein structure which sometimes may destabilize it to accelerate or to inhibit protein aggregation. Coumarin is a widely used fluorescent dye with several biological applications. Different substituents (electron-donating and electron-withdrawing) at different positions of the coumarin moiety can influence its molecular volume, physical and chemical properties. Here we investigate the effect of such substituents of coumarin on the aggregation of a model protein, beta-lactoglobulin ( $\beta$ -lg) through a multi spectroscopic approach. It was observed that coumarin methyl ester with an 8-hydroxyl group can inhibit the  $\beta$ -lg aggregation. This compound can bind the hydrophobic site of beta-lactoglobulin and stabilize a particular protein conformation through the formation of hydrogen bond and hydrophobic interactions. Thus a properly designed compound can inhibit protein–protein interactions through protein–small molecule interactions. Other coumarinoid compounds also are effective in the prevention of thermal aggregation of  $\beta$ -lg.

Received 16th February 2022  
Accepted 15th May 2022

DOI: 10.1039/d2ra01029a

rsc.li/rsc-advances

## Introduction

The formation of insoluble amyloid fibrils from normal soluble proteins is well known. Amyloid fibrils are impervious to degradation.<sup>1</sup> Proteins can form amyloid fibrils and each case brings a different characteristic disease. Aggregation of A $\beta$ ,  $\alpha$ -synuclein, or prion proteins causes neurodegenerative brain disorders Alzheimer's disease, Parkinson's disease, or mad cow disease, respectively. It is also found that diseases like diabetes type 2 are disorders due to amyloid fibril formation of insulin.<sup>1</sup> Since amyloid fibrils are insoluble in physiological conditions, they can deposit around the cell and tissues and cause a pathogenic effect.<sup>2</sup> Aggregation of such proteins gives very stable systems and facilitates the process. Structurally, fibrillar assemblies are predominantly cross- $\beta$  conformation of the proteins. Interestingly, the formation of fibrils is independent of protein size, shape, and sources. Recently, hydrophobins, curli, and melanosomes are identified as the expression of functional amyloidogenesis.<sup>1</sup>

To prevent the amyloid fibrils formation, a number of therapeutic strategies have been developed. Site-specific

glycosylation of protein<sup>3</sup> and protein engineering<sup>4</sup> are of some example of prevention techniques. Most of the proteins have a very stable conformational structure in fibrillar form because it is in a global free-energy minimum.<sup>5–7</sup> Therefore, once a protein starts partial degradation to form a fibril, it is very hard to stop the process. Stabilization of the native conformer of a protein can slow down the partial degradation of protein and can deem fibrillation.<sup>8</sup> It is the most acceptable therapeutic strategy to prevent fibrils formation now. Therefore, the design of new anti-fibrillating molecules is in demand.

Coumarin, an aromatic heterocyclic lactone compound, is an important natural product found in many plants. Coumarin derivatives or coumarinoids have a large family containing thousands of compounds. They have very interesting photophysical,<sup>9</sup> biological, and medicinal<sup>10</sup> properties. Coumarin absorbs light at  $\sim$ 280 nm wavelength and shows fluorescence property by the emission at 410 to 470 nm. This photophysical property is very much tunable with the substituents attached to the moiety.<sup>11</sup> For this reason, these compounds are widely used as dyes. Some coumarinoids were designed for blue-green tunable organic laser dyes.<sup>11</sup>

Whey contains an important lipocalin protein, *i.e.*  $\beta$ -lactoglobulin ( $\beta$ -lg), which is of immense interest due to its nutritional and small molecule carrier properties.<sup>12</sup> Structurally, the protein is  $\beta$ -sheet enriched (eight anti-parallel  $\beta$ -sheets forms a barrel-like structure) and forms self-assembly upon thermal exposure. The protein can be isolated and purified in high yield

<sup>a</sup>Department of Chemistry, Jadavpur University, Kolkata 700 032, India. E-mail: uhalder2002@yahoo.com

<sup>b</sup>Department of Chemistry, Lady Brabourne College, Kolkata 700017, India

† Electronic supplementary information (ESI) available. See <https://doi.org/10.1039/d2ra01029a>



following the method described by Aschaffenburg and Drewry, 1957.<sup>13</sup> Hence it is a very good model protein for the protein aggregation studies.<sup>14</sup>

A 4-hydroxycoumarins derivative Warfarin can interact with proteins to inhibit their aggregation and it is used as an anti-coagulant of blood.<sup>15</sup> 4-Hydroxycoumarins are also anticoagulants and antagonists of vitamin K.<sup>16</sup> It was observed that the substituents of coumarin have a substantial effect on the aggregation process of the amyloid- $\beta$  protein.<sup>17</sup> Some coumarinoids show inhibition of insulin fibrillation.<sup>18</sup> Some coumarin hybrid molecules are also be designed as a multi-targeting agent to stop the fibrillation process in neurodegenerative disorders.<sup>19</sup> All these facts encourage us to investigate some polyphenolic coumarinoids as anti-fibrillating agents. Here, we have synthesized and characterized some polyphenolic coumarinoids and applied them to check their anti-fibrillation power on the model protein  $\beta$ -lg.

## Results and discussion

### Synthesis of coumarinoids

In this study, all the coumarin derivatives was synthesized except 4-hydroxycoumarins (3) which were collected from commercial source and used without further purification. Kayal *et al.*, showed that polyhydroxy benzenes can be reacted with electron-deficient alkynes to produce polyhydroxycoumarinoids (SM1–SM4) with the help of 5 mol% CuO in refluxing toluene.<sup>20</sup> Here, this method was used for the synthesis of different polyhydroxycoumarinoids and it has been shown in the Fig. 1. All these compounds were well characterized and used in the protein aggregation experiments.

It is interesting to note the distribution of hydroxyl groups around the coumarin nucleus in the compounds under investigation. In compound 3, the hydroxyl group at C4 position. In the case of SM1, one methyl carboxylate is attached at C4 position and OH is shifted to the C5 position. The OH group is at C8 and C7 carbon in SM2 and SM4, respectively. SM3

contains two hydroxyl groups at C5 and C7 positions. Here, we investigate the effect of hydroxyl groups along with methyl carboxylate group on the protein aggregation.

### UV-spectral characterization

UV spectroscopy is employed to get an intuition of structural change of  $\beta$ -lg due to interaction with small molecules.<sup>21</sup> Here we used absorption spectroscopy to investigate the structural change of  $\beta$ -lg in the presence of coumarin derivatives. Due to the presence of Trp and Tyr moiety a sharp characteristics peak is observed at  $\lambda_{\max}$  280 nm for  $\beta$ -lg. Coumarin derivatives have also light absorption properties and have  $\lambda_{\max}$  around 270 nm (for 3, SM1, SM2, and SM4) and 350 nm (for SM3) which is presented in Fig. S1a.†

In the presence of methyl 4-hydroxy-chromen-2-one (3) and methyl 8-hydroxy- 2-oxo-2H-chromene-4-carboxylate (SM2), the absorption intensity become lower than that of native  $\beta$ -lg and higher than that of heat-treated  $\beta$ -lg UV spectra (Fig. 2). However,  $\beta$ -lg with methyl 5-hydroxy-2-oxo-2H-chromene-4-carboxylate (SM1), methyl 5,7-di-hydroxy-2-oxo-2H-chromene-4-carboxylate (SM3), and methyl 7-methoxy-2-oxo-2H-chromene-4-carboxylate (SM4) shows a clear bathochromic shifts with low-intensity peaks compared to native. The contribution of the coumarin molecules in the aforesaid absorption spectra can be eliminated by their addition in the reference cell along with sample cell (both the cell have the same concentration of coumarin derivatives). In this experiment, we found only single peak at 280 nm for all coumarin derivatives (Fig. S1b†). The intensities of the spectra of the sample containing protein with coumarin derivatives are higher than that of native and heat-treated protein. All these observations indicate the probability of interactions of the small molecule with the protein  $\beta$ -lg.

### Intrinsic fluorescence

The fluorescence technique, a highly effective and sensitive method, is widely used to monitor the structural change of

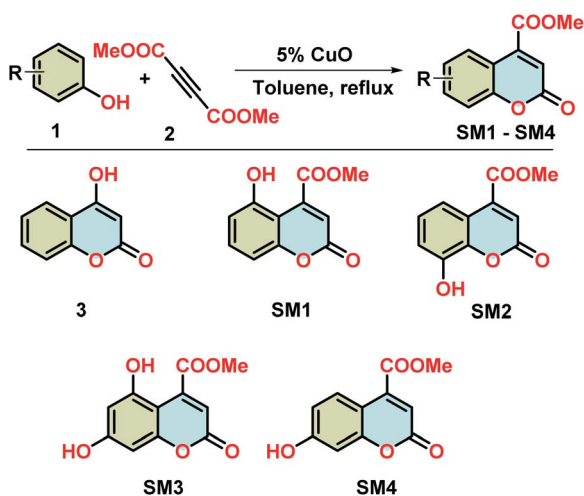


Fig. 1 Synthesis of coumarin derivatives.

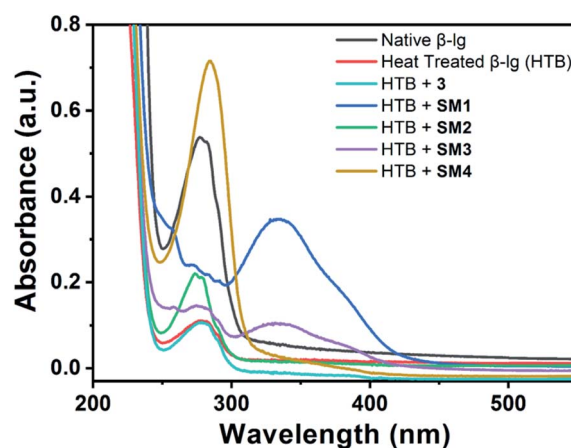


Fig. 2 Absorption spectra of native  $\beta$ -lg and  $\beta$ -lg incubated at 78 °C for 1 h in the absence and presence of different coumarinoid molecules.

protein and its interaction with the small molecules. Generally, Trp and Tyr are the amino acid residues that absorb the light of corresponding wavelengths and show the fluorescence properties for most of the proteins.  $\beta$ -lg has four Tyr (Tyr20, Tyr42, Tyr102, and Tyr99) and two Trp (Trp19 and Trp61) residues which are responsible for the intrinsic fluorescence of the protein.<sup>22</sup> It can be used to investigate the alteration of the polarity around the microenvironment of the fluorophore due to the structural change of beta-lactoglobulin. In the case of aggregation of  $\beta$ -lg, solvent exposure of fluorophores (mainly tryptophan) decreases which is reflected in their emission spectra with the change in fluorescence intensity. Here, aggregation of  $\beta$ -lg was investigated in the presence of coumarin derivatives.

The intrinsic fluorescence of  $\beta$ -lg increases after heating at 78 °C for 1 h due to the aggregation of the native protein (Fig. 3). In the case of **SM2** and **3**, the fluorescence intensities are slightly higher and lower with respect to heat-treated  $\beta$ -lg, respectively. Under the same aggregation conditions, **SM1** and **SM3** show higher fluorescence intensities than native  $\beta$ -lg but lower than heat-treated  $\beta$ -lg. However, in the presence of **SM4**, the intensity is lowered compared to native  $\beta$ -lg.

Thus coumarin derivatives interact with  $\beta$ -lg and are able to change the conformation of the protein during its thermal exposure. It should be mentioned here that compound **SM4** can interact with  $\beta$ -lg in such a way that Trp residue may expose more in the solvent. It may be the reason for the decrease in fluorescence intensity of  $\beta$ -lg with **SM4** under aforesaid conditions.

### Aggregation of $\beta$ -lg identification and quantification of the aggregates by ThT assay

Thioflavin T (Th-T), a benzothiazole dye, is a good fluorescent ligand that selectively binds with the hydrophobic site of the fibrillar aggregates of the protein leading to an increase in fluorescence intensity at around 480 nm upon excitation at 480 nm.<sup>23</sup> Upon heating at 78 °C, the native  $\beta$ -lg gets aggregated

which can be measured in terms of intensity of the Th-T spectra. Here, all the other heat-treated  $\beta$ -lg samples with different coumarin derivatives produced different Th-T emission intensities which are proportional to the amount of aggregates formed in the different protein solutions. Therefore, lower intensity of the Th-T will indicate a lower degree of aggregate formation due to the presence of effective anti-fibrillating coumarin derivatives. Determination of equivalent molar ratio of the compounds against protein through UV and fluorescence spectra is very difficult as both of them (protein and **SMs**) have absorbance and emission peaks at the same region. In such case, we have monitored the change of fluorescence intensity of Th-T in the presence and absence of coumarin derivatives with different molar ratio at a fixed [BLG] which is given in Fig. S2.† The study showed that 1 : 1 protein and SM compound ratio is most effective for protein aggregation inhibition. In the Fig. 4, it shows a comparative study of the aggregation patterns of native and heat-treated  $\beta$ -lg in the absence and presence of different coumarin derivatives (1 : 1) at pH 7.4 in Th-T assay.

Owing to self-assembly formation, the heat-treated  $\beta$ -lg shows the highest Th-T intensity as shown in the Fig. 4. The  $\beta$ -lg in the presence of **3** under identical heating conditions exhibits slightly lesser intensity in Th-T fluorescence measurement than heat-treated  $\beta$ -lg alone. However, when  $\beta$ -lg was incubated at 78 °C separately with other coumarin compounds **SM1**, **SM2**, **SM3**, and **SM4** very much decreased intensities of Th-T fluorescence were observed due to the formation lower  $\beta$ -lg aggregates. Therefore, synthesized coumarin derivatives can act as effective anti-fibrillating agents to inhibit the oligomerization of  $\beta$ -lg. In this case, the inhibition of aggregation of coumarin derivatives follows the order as **SM2** > **SM4** > **SM3** > **SM1** > **3**.

### ANS-fluorescence study to monitor the hydrophobicity changes

1-Anilinonaphthalene-8-sulfonate (ANS), a fluorescent probe, can bind at the surface of protein aggregates through the

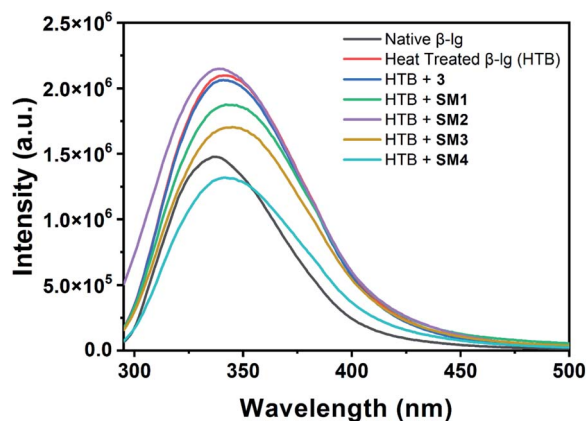


Fig. 3 Intrinsic fluorescence spectra of native  $\beta$ -lg and  $\beta$ -lg incubated at 78 °C for 1 h in the absence and presence of different coumarin derivatives (protein: coumarin derivatives = 1 : 1).

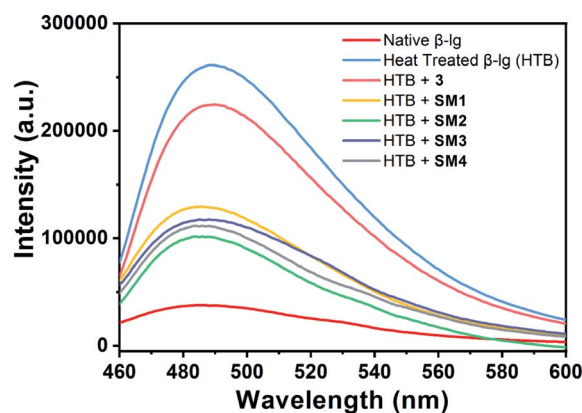


Fig. 4 Th-T ( $\lambda_{\text{ex}}$  = 440 nm and  $\lambda_{\text{em}}$  = 485 nm) assay of native  $\beta$ -lg and heat-treated  $\beta$ -lg (incubated at 78 °C for 1 h) in the absence and presence of different coumarin compounds (1 : 1) at pH = 7.4, excitation wavelength was set at 440 nm and emission wavelength was 480 nm.



hydrophobic and electrostatic interaction at the hydrophobic site.<sup>24</sup> To monitor hydrophobic interactions involved in the aggregation processes, ANS fluorescence experiment was performed.

The protein,  $\beta$ -lg, has two potential binding sites for binding with hydrophobic small molecules. The first site is the inner side of the beta-barrel and the second site is at the channel between the barrel and the alpha helix. The dye shows fluorescence emission around 480 nm with an increase of fluorescence intensity after binding with the hydrophobic site of the protein.<sup>25</sup>

The heat exposed  $\beta$ -lg (78 °C, 1 h) showed an enhanced ANS fluorescence intensity at around 480 nm. This increase in fluorescence intensity may be attributed to more access of ANS to the hydrophobic patches present in heat treated  $\beta$ -lg compared to native  $\beta$ -lg during its aggregation (Fig. 5). The incubation of the coumarin derivatives with  $\beta$ -lg slows down the aggregation process since the ANS intensity in each case is lower than that of the heat-treated sample. Additionally, it may be mentioned here that these aggregates have lower surface hydrophobicity. Therefore, the hydrophobic pockets of  $\beta$ -lg are opened up during thermal exposure implying a conformational change of native protein.

We obtained significant result when  $\beta$ -lg was incubated with **SM2** at 78 °C. The ANS fluorescence intensity was found to decrease considerably and it is very closer to that of native  $\beta$ -lg, indicating least disclosure of hydrophobic loops of  $\beta$ -lg demonstrating least binding of ANS, and thus **SM2** very efficiently decreased protein-protein interactions and thus inhibiting the thermal aggregation of  $\beta$ -lg.

For incubation of  $\beta$ -lg with **3**, **SM1** and **SM3**, such spectral changes are though very close to each other but ANS fluorescence intensities have been reduced to almost 55% compared to that of heat-treated  $\beta$ -lg alone. This suggests lesser opening of hydrophobic loops resulting decreased protein-protein interactions in the presence of **3**, **SM1** and **SM3** although greater ANS

bindings and hence increased hydrophobicities compared to **SM2** were observed. Therefore, it may be concluded that the  $\beta$ -lg fibrillation proceeds through the exposure of hydrophobic sites to the solvent and the binding of coumarin derivatives to the hydrophobic site of the protein can stabilize it in such a way that the protein cannot proceed to the fibrillation mechanism. Therefore, lower ANS intensity indicates a higher ability of stabilization of protein conformation by coumarin derivatives. It is found that the order of stabilization is **SM2** > **SM4** > **SM3** > **SM1** > **3**. This result supports the Th-T data given above.

### Rayleigh light scattering (RLS) study

Protein aggregation can also be investigated with the help of RLS measurements. The scattering of light is increased in the presence of colloidal particles in the medium. Therefore, higher protein aggregates can scatter light efficiently over the smaller aggregates. In this study, RLS data were collected after incubation of  $\beta$ -lg solutions at 78 °C for 1 h in absence and presence of coumarin derivatives. Our result as shown in Fig. 6 indicates that maximum scattering intensity was observed with heat-treated  $\beta$ -lg in absence any coumarin derivative. On thermal denaturation, the structure of a protein is lost and it forms maximum aggregates. Decreased RLS intensities were noted in the presence of different coumarin derivatives indicating the formation of smaller  $\beta$ -lg aggregates. Thus it is worth to point out that coumarin derivatives maintain the structural integrity of the protein during the thermal denaturation. It was found that **SM2** is superior to other coumarin derivatives in the inhibition of protein-protein interactions during thermal exposure as the minimum RLS intensity value (closer to that of native  $\beta$ -lg) was obtained (Fig. 6). Lowering in RLS intensities confirms the smaller aggregate formation during thermal incubation. In our present study the order of inhibition of thermal aggregation of  $\beta$ -lg by the coumarin derivative is the same as that obtained with other experiments and it follows **SM2** > **SM4** > **SM3** > **SM1** > **3**.

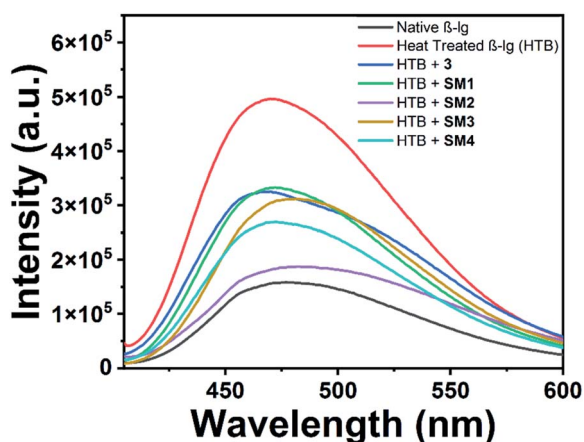


Fig. 5 ANS-fluorescence emission spectra of native  $\beta$ -lg and  $\beta$ -lg incubated separately at 78 °C for 1 h in the absence and presence of different coumarin derivatives (1 : 1) at pH = 7.4.  $\beta$ -lg concentrations throughout all emission experiments were kept at 0.25 mg mL<sup>-1</sup>. Results were the mean of three different experiments.

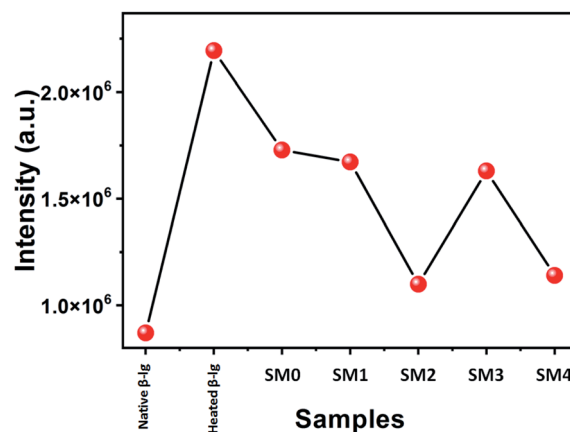


Fig. 6 Rayleigh light scattering data of  $\beta$ -lg at native form and  $\beta$ -lg incubated at 78 °C for 1 h in the absence and presence of different coumarin derivatives (1 : 1) at pH = 7.4.



### Dynamic light scattering (DLS) measurements

Dynamic light scattering (DLS) was unambiguously used to identify the heat-induced oligomers of  $\beta$ -lg and also to measure their hydrodynamic size. The size distribution profile of the native  $\beta$ -lg, its heat-treated form without and with the different coumarin derivatives were investigated and have been shown in Fig. 7. The size distribution curves of heated (78 °C, 1 h)  $\beta$ -lg with and without coumarin compounds showed the formation of different sized protein aggregates. The hydrodynamic radius of native  $\beta$ -lg was ranging from 12 nm to 50 nm and its size was enhanced to 1250–3200 nm range when the protein was incubated at 78 °C for 1 h, clearly indicating the formation of large  $\beta$ -lg aggregates having greater light scattering effect. In presence of different coumarin derivatives the scattering intensity of  $\beta$ -lg solution decreased. The sizes of protein aggregates were decreased in the presence of **3** and it was in the region 1500–2750 nm. Minimum hydrodynamic radius was noted during incubation with **SM2**. The size of the aggregates decreased minimally in the range of 100–450 nm and aggregates with smaller diameter became prominent during thermal incubation with the other coumarin molecules. The hydrodynamic radii of protein aggregates in presence of coumarin derivatives have been found to follow the order **3** > **SM1** > **SM3** > **SM4** > **SM2**. Therefore, it is interesting to note that all these coumarin compounds are potent inhibitors of  $\beta$ -lg fibrillation and the order of the ability of inhibition by the coumarin derivatives is **SM2** > **SM4** > **SM3** > **SM1** > **3** (Fig. 7). This result also corroborated with AFM imaging of different  $\beta$ -lg aggregates.

### Monitoring the changes in secondary structure of $\beta$ -lg during thermal incubations with circular dichroism spectroscopy

Far-UV CD technique has been employed to investigate the potential effect of different coumarinoid compounds used in this study on the secondary structural transformation of  $\beta$ -lg. The  $\beta$ -lg solutions were incubated with or without different

coumarin derivatives at 78 °C for 1 h and the different secondary structures were determined by CD spectroscopy. CD measurements were carried out by scanning the spectra in the region 190–250 nm and represented in Fig. 8. Native  $\beta$ -lg showed two negative bands at 208 nm and 215 nm. These two bands of  $\beta$ -lg represented the existence of ordered secondary structure that contained  $\alpha$ -helix and  $\beta$ -sheet.<sup>26</sup> The oligomeric structure of incubated  $\beta$ -lg at 78 °C is found to have greater amount of beta structural contents ( $\sim 61\%$ ) with lesser alpha helical structure ( $\sim 9.0\%$ ) than the native (Table S1, see ESI†). This data provided the information regarding the formation of greater  $\beta$ -sheet structures linked with the thermal aggregation of the protein. The CD spectrum of  $\beta$ -lg also showed a significant shift in the band positions. Then we analysed the change of secondary structure of heat-treated  $\beta$ -lg in presence of different coumarin compounds. With **3**, a small change of peak position with negative ellipticity value differing from heated  $\beta$ -lg was observed. CD spectra of  $\beta$ -lg in presence of **SM1** showed lower MRE values at 215 and 207 nm. In both the cases lesser  $\beta$ -structures has been formed compared heat-treated  $\beta$ -lg alone indicating structural transitions leading to the disaggregation in the presence of **3** and **SM1**. It is interesting to mention that the shape of CD signal of  $\beta$ -lg in presence of the coumarin derivative **SM2** is similar to that of the native though decreased negative ellipticities are observed in the vicinity of 208 nm and 215 nm. The difference in MRE values could be related to the structure of the derivatives. The amount of different  $\beta$ -structures decreased most significantly compared to heat-stressed  $\beta$ -lg alone (Table S1†) showing maximum inhibitory power **SM2** against the thermal aggregation of  $\beta$ -lg. Other two coumarin derivatives **SM3** and **SM4** displayed almost similar CD spectra in this region but CD results revealed that **SM4** is more potent than **SM3** in the suppression of fibrillation of  $\beta$ -lg. Hence all the coumarin compounds used in this study showed their effectiveness in the suppression of thermal aggregation of  $\beta$ -lg and the order of their inhibition is **SM2** > **SM4** > **SM3** > **SM1** > **3**. The calculation of secondary structural changes of  $\beta$ -lg in the

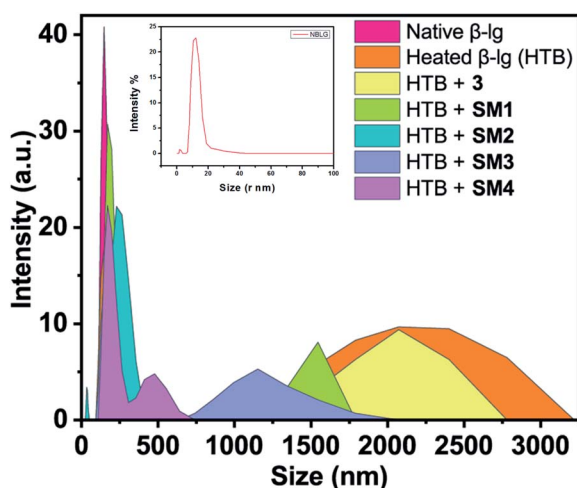


Fig. 7 Number particle size distribution spectra in DLS studies of  $\beta$ -lg at native form and  $\beta$ -lg incubated at 75 °C for 1 h in the absence and presence of different coumarin derivatives (1 : 1) at pH = 7.4.

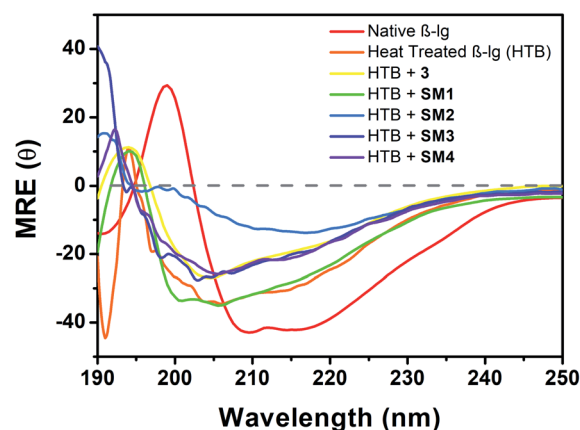


Fig. 8 Far-UV CD spectra (190–250 nm) of native  $\beta$ -lg, heat treated  $\beta$ -lg (78 °C, 1 h), and  $\beta$ -lg incubated (78 °C, 1 h) in the presence of different coumarin derivatives (1 : 1) at pH = 7.4 showing secondary structural changes during thermal aggregation.



absence and presence of different coumarin compound was done by CDNN 2.1 software and shown in Table S1.†

### Morphological studies with atomic force microscope (AFM)

To gain more insight, atomic force microscopy was also employed; it has been proved to be a powerful tool in the study of fibril formation.<sup>27</sup> AFM analysis was performed to visualize the extent of disruption of  $\beta$ -lg samples aggregated alone or with coumarin derivatives at molar concentration ratios of 1 : 1.

The morphology of the  $\beta$ -lg aggregates in different conditions is shown in Fig. 9. It is revealed that the three-dimensional AFM images of the aggregates are globular, not fibrillary. The AFM image of  $\beta$ -lg shows that it is smaller globular particles (Fig. S3†). Large globular aggregates of  $\beta$ -lg formed after incubation of the  $\beta$ -lg solution alone at 78 °C for 1 h (Fig. 9a). During thermal incubation the  $\beta$ -lg monomers are swelled owing to change of its conformation, forming the aggregates.

To investigate the effect of different coumarin derivatives on the aggregation mechanism, the  $\beta$ -lg sample was co-incubated at 78 °C for 1 h in the presence of coumarin derivatives at a molar concentration ratio 1 : 1. The compound 3 was found to be inefficient in the inhibition of protein aggregation because the nature and size of aggregates are very similar to the  $\beta$ -lg aggregates obtained after heat treatment (Fig. 9b). A similar type of results were obtained in the case of **SM1**, large globular type aggregate (Fig. 9c). But the AFM image analysis clearly demonstrates that the larger and numerous globular aggregates of  $\beta$ -lg were disappeared when it was thermally incubated with the coumarin compound **SM2** (Fig. 9d). Here, the density of the aggregates was very low. Thus it was found to be most efficient to inhibit and arrest the aggregation of  $\beta$ -lg. However, **SM3** is

less efficient than that of both **SM2** and **SM4** but better than other compounds (Fig. 9e). The size of the aggregate particles formed with **SM3** is sufficiently smaller than with heat-treated  $\beta$ -lg (Fig. 9a) or with heat-treated  $\beta$ -lg in presence of 3 (Fig. 9b). Thus **SM3** is also efficient to suppress the formation larger globular aggregates of  $\beta$ -lg. The AFM studies also support the order of inhibition efficiency of coumarin derivatives obtained in all the previous experiments and the order is **SM2** > **SM4** > **SM3** > **SM1** > 3.

### Docking studies

The small molecules can interact with the protein and can stabilise the native protein conformation and it may be attributed to the anti-protein aggregation effect of these small molecules. To understand the effect of coumarin derivatives on the native structure of  $\beta$ -lg, docking studies were performed. It is found that the binding energies ( $\Delta G^\circ$ ) of 3, **SM1**, **SM2**, **SM3** and **SM4** are  $-5.6$ ,  $-5.8$ ,  $-7.6$ ,  $-6.3$ , and  $-6.9$  kcal mol<sup>-1</sup> respectively. The result indicates that the order of stabilization by these molecules is **SM2** > **SM4** > **SM3** > **SM1** > 3. This order of stabilization of  $\beta$ -lg structure with these molecules is corroborated with their protein-aggregation inhibition order. Therefore, the coumarin molecules can stabilize the  $\beta$ -lg conformation and locked a protein structure to inhibit the protein-protein interactions, playing the key role in the protein aggregation pathway.

Analysis of the docking results can provide an insight of the molecular interactions required for the freezing a conformation of protein. The **SM2** binds at the narrow end of the barrel of the  $\beta$ -lg (Fig. 10a). The cavity in this region encapsulates the molecule (Fig. 10b). It was observed that the methoxy oxygen

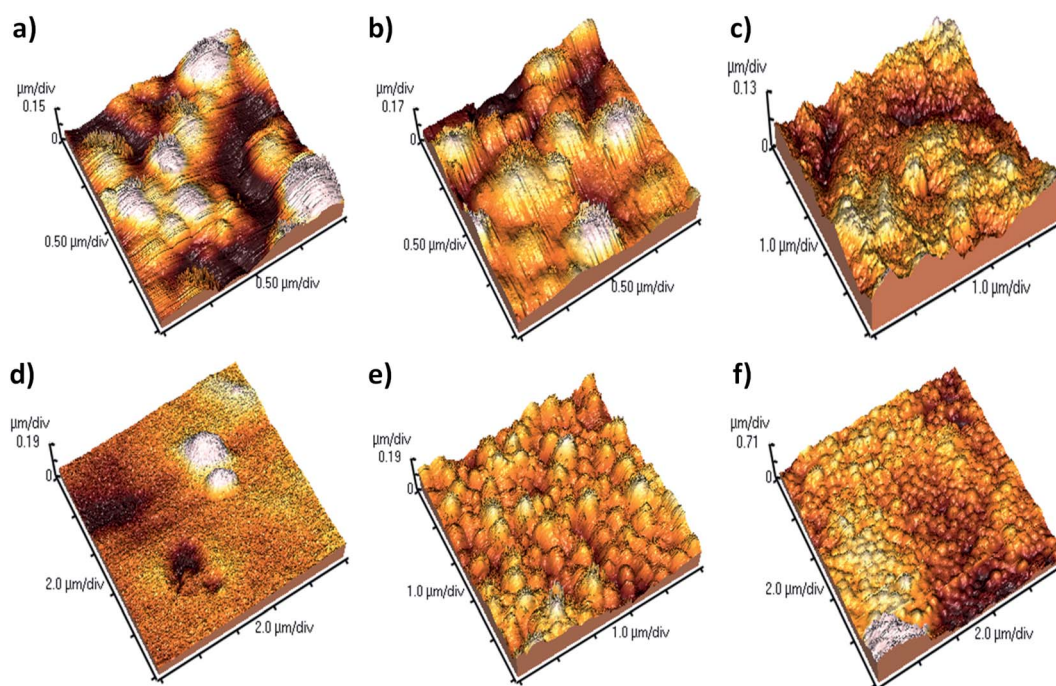


Fig. 9 AFM images representing (a) the aggregate morphologies of heat treated  $\beta$ -lg and (b–f) heat treated  $\beta$ -lg in the presence of coumarin derivatives: (b) with 3, (c) with **SM1**, (d) with **SM2**, (e) with **SM3**, (f) with **SM4**.

atoms and the hydroxyl group are involved in the hydrogen bonding with N88, N98 and S116 amino acid residues. The non-conventional hydrogen bonding was also observed between ring C=O of coumarin and S116. The methyl of methoxy group found to be interacted with L39 through hydrophobic interactions (Fig. 10c). Docking studies reveals that the positions of OH groups play an important role in their protein binding. The OH groups at C4 and C7 are unable to involve hydrogen bonding with amino acid residues. However, hydroxyl groups at C4, and C5 can interact with the amino acid residues in their corresponding active site (Fig. S4 and S5†). Therefore, hydrogen bonding stabilization of protein–SM complexes can influence the protein aggregation.

The protein can exist as dimer in native state. In this quaternary form of the protein have one additional binding pocket (Fig. S6 and S7a†). It is possible that coumarin derivative able to bind this site to show aforesaid effect. The molecular docking was performed to find such binding possibility. In this case, energy minimized dimeric protein is used for docking. It is found that the binding energies ( $\Delta G^\circ$ ) of 3, **SM1**, **SM2**, **SM3** and **SM4** are  $-3.2$ ,  $-3.9$ ,  $-5.2$ ,  $-4.3$ , and  $-4.7$  kcal mol $^{-1}$ , respectively. These binding energies are quite lower than that of the values obtained from monomeric form of the protein. All the docking poses are shown in the Fig. S7(b)–(f)†.

## Experimental

### Synthesis of coumarin derivatives<sup>20</sup>

To a round bottomed flask a mixture of resorcinol (110 mg, 1.0 mmol) and dimethyl acetylenedicarboxylate (170 mg, 1.2 mmol) were taken in 1.3 mL dry toluene and stirred magnetically in

a 10 mL round bottom flask. Then 4 mg CuO (0.05 mmol) catalyst was added to the mixture and allowed the stirring for 3 h at 110 °C. The degree of conversion into the products was noticed by thin layer chromatography. The solvent of the reaction mixture was removed under low pressure, and the pure product was obtained after column chromatography with the help of silica gel (100–200 mesh). The pure compounds were characterized using  $^1\text{H}$  NMR and  $^{13}\text{C}$  NMR spectroscopy. All the data are given in the ESI.†

### Preparation and purification of beta-lactoglobulin<sup>13</sup>

Bovine  $\beta$ -lg was isolated and purified from cow milk as described by Aschaffenburg and Drewry.<sup>13</sup> The final product was lyophilized and stored at 4 °C. For spectroscopic sample preparation,  $\beta$ -lg was weighed and dissolved in 0.01 M Na-phosphate buffer pH 7.4 solution containing 2% ethanol. Protein stock solutions were prepared using phosphate buffer pH-7.4. Since the extinction coefficient of  $\beta$ -lg ( $0.96 \text{ mg}^{-1} \text{ mL}^{-1} \text{ cm}^{-1}$  at 280 nm) is known, different concentrations of protein samples were prepared by dissolving  $\beta$ -lg samples in Milli-Q-water and then measuring the O.D. at 280 nm.

### UV-visible spectroscopy

Utilizing UV-visible JASCO V700 spectrophotometer (Model no. V-730, Serial no. B184461798 and JASCO Spectra Manager software), absorption spectra were recorded to check the binding affinity and binding constant at room temperature (25 °C). To perform this experiment two PerkinElmer quartz cell of path length of 1 cm were used for both reference and samples. The intensity vs. wavelength spectra for the absorbance measurement was recorded over the wavelength range 200–600 nm. For reference cell 10 mm phosphate buffer of pH 7.4 were taken. Concentration of the sample solutions were 13  $\mu\text{M}$ .

### Intrinsic fluorescence study

Fluorescence measurements were carried out using Horriba Fluorometer (Model: FLUOROMAX-4C, Serial no. 1734D-4018-FM). Stock solution of  $\beta$ -lg and others solution of 13  $\mu\text{M}$  were taken in a fluorescence quartz cell of path length of 1 cm and excited at 295 nm. Emission spectra were recorded in the range of 300 to 550 nm. Excitation and emission slit were set at 5 nm. Data were recorded at a scan rate of 100 nm s $^{-1}$ .

### Thioflavin T (Th-T) fluorescence

Th-T binds with the aggregates of  $\beta$ -lg and other amyloid fibrils. After binding it shows enhanced fluorescence at 480 nm. For this experiment stock  $\beta$ -lg samples of 54.3 mM were mixed with 3.13 mM Th-T solution. The assay solution was excited at 450 nm (ref. 28) and the emissions were measured over the range 460 to 600 nm using Horriba Fluorometer (Model: FLUOROMAX-4C, Serial no. 1734D-4018-FM) and Fluoromax Software. Slit widths for both excitation and emission were kept at 5 nm.

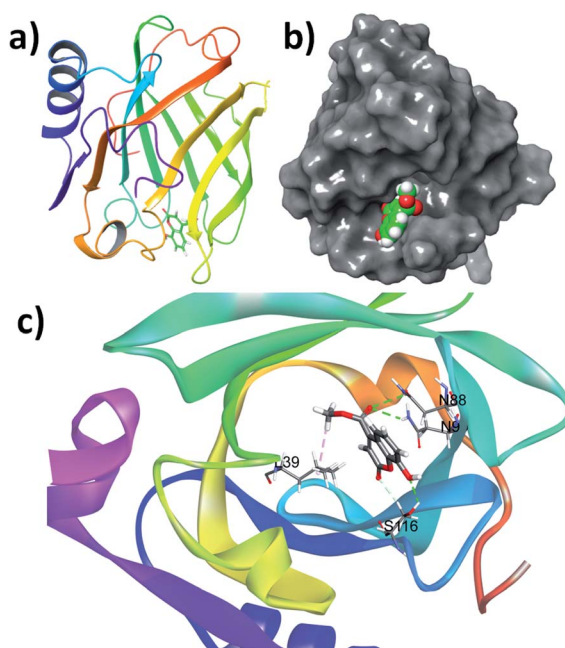


Fig. 10 (a) The structures of the most stable  $\beta$ -lg–coumarin **SM2**, bind at the terminal of the barrel, (b) binding of **SM2** at the hydrophobic pocket, (c) different non-covalent interactions in the binding site of  $\beta$ -lg with **SM2**.





### ANS-fluorescence study to monitor the hydrophobicity change

Hydrophobicity of protein molecules were measured using fluorescent probe which binds with the hydrophobic packets of protein surface.<sup>25</sup> A well-known polarity sensitive probe is 1-anilinonaphthalene-8-sulfonate (ANS). To measure the hydrophobicity a stock solution of ANS is prepared and added to the each samples (2 mL volume). The final concentration of ANS in each sample is maintained 30  $\mu\text{M}$ . Fluorescence spectra were measured at 390 to 550 nm after excitation at 380 nm and emission spectra were recorded using Shimadzu spectrofluorometer (Shimadzu 5301 PC). Path length was 1 cm. Excitation slit was 5 nm and emission slit was also 5 nm.

### Raleigh light scattering (RLS)

The formation or change in the presence of turbidity or aggregates after the incubation of  $\beta$ -lg in absence and presence of different coumarin samples (3-**SM4**) with respect to the native  $\beta$ -lg were quantitatively measured using Raleigh light scattering study. For this study samples were excited at 350 nm and then emission intensity were recorded at 350 nm using Horriba Fluorometer (Model: FLUOROMAX-4C, Serial no. 1734D-4018-FM) and Fluoromax Software. Samples were prepared using 10 mM phosphate buffer (pH = 7.4). 2 mL 13  $\mu\text{M}$  solution of each samples were taken in a quartz cell of 1 cm path length for this experiment and excitation and emission slit were 5 nm.

### Analysis of secondary structures by CD spectroscopy

Using Jasco spectropolarimeter (J-815) (Jasco, Tokyo, Japan) CD spectra of  $\beta$ -lg, heat treated  $\beta$ -lg and heat treated  $\beta$ -lg in presence of different coumarin compounds were recorded with the help of Jasco Spectra Manager Software. For this experiment in the far UV region (190–260 nm), each sample containing 13.6  $\mu\text{M}$   $\beta$ -lg was taken in a PerkinElmer quartz cell of path length of 0.2 cm and then data was recorded in the inner nitrogen atmosphere of the instrument at 190 nm to 260 nm. Scan speed was 100 nm  $\text{min}^{-1}$  and temperature was 30  $^{\circ}\text{C}$ . The results were expressed as mean residual ellipticity (MRE) in  $\text{deg cm}^2 \text{dmol}^{-1}$  which is defined as:

$$\text{MRE} = \theta_{\text{obs}} (\text{mdeg}) / 10 \times n \times C_p \times l$$

where  $\theta_{\text{obs}}$  is the CD in millidegree,  $n$  is the number of amino acid residues in one subunit (162 for  $\beta$ -lg),  $l$  is the path length of the cell in centimeters and  $C_p$  is the molar fraction of proteins.

Spectra were recorded using Jasco Spectra Analysis tool. And secondary structural elements were calculated from CDNN 2.1 software.

### Dynamic light scattering (DLS)

Dynamic light scattering (DLS) study is used to determine the size of proteins, nucleic acids, and complexes or to monitor the binding of ligands. Also, diffusion of tiny particle of nano sized range alters the intensity of the scattered light. DLS studies are also used to determine the presence of different molecules and supramolecules as it is very sensitive to particle size.<sup>29</sup> Using

Zetasizer Nanos (Malvern Instrument, U.K.) equipped with 633 nm laser and using 2 mL rectangular helma cuvette of 1 cm path length DLS Measurements were done at 20  $^{\circ}\text{C}$  taking 250  $\mu\text{L}$  of samples ( $\beta$ -lg, heat treated  $\beta$ -lg, and heat treated  $\beta$ -lg in presence of different coumarin compounds) in 1.75 mL 3 mM glycine-KOH buffers of pH 7.4. The time-dependent auto correlation function was acquired with twelve acquisitions for each run.

### Morphological study with AFM

For this experiment AFM grid slides is prepared. For grid preparation drop casted solution of different samples (each containing 5  $\text{mg mL}^{-1}$   $\beta$ -lg) in the surface of a glass slide and then sample is spread all over the slide and then dried overnight for the observation. AFM microscope image of  $\beta$ -lg, heat treated  $\beta$ -lg and  $\beta$ -lg incubated at 78  $^{\circ}\text{C}$  in the presence of different coumarin compounds were developed using VEECO DICP II autoprobe (Model AP 0100).

### Molecular docking study

The AutoDock 4.2.0 based docking studies of coumarin derivatives molecule with  $\beta$ -lg (1BSY) were carried out. The structure of coumarin derivatives used in docking after minimized its energy by DFT optimization using Gaussian 09W. Lamarckian genetic algorithm (LGA) was utilized for molecular docking. In this calculation,  $126 \times 126 \times 126$  grid box was used.

## Conclusions

In summary, the work presents application of some coumarin derivatives for the inhibition of  $\beta$ -lg aggregation. Protein aggregation can occur due to protein-protein interaction of a particular conformation of a protein. The synthesized coumarin derivative can stabilize a protein conformer so that it unable to reach the conformation essential for protein-protein interaction. We have tested five coumarin derivatives to prevent the protein aggregation. The results showed that the coumarin derivatives have inhibition ability in the order **SM2** > **SM4** > **SM3** > **SM1** > **3**. In the molecule **SM2**, one hydrogen bond donor (OH) and two hydrogen bond acceptor (ring O and C=O) groups are in a row. This structural feature of the molecule may help to fit the molecule in the barrel of the protein through hydrogen bonds. This makes **SM2** the best inhibitor. We utilised UV-visible, fluorescence, and CD spectroscopy, Raleigh light scattering, dynamic light scattering (DLS) and AFM techniques to determine the order and to understand the mechanism of inhibition of protein aggregation. Therefore, the work showed the protein aggregation through protein-protein interactions can be inhibited through locking of a protein at its native-like conformation using protein-small molecule interactions.

## Author contributions

HP performed most of the experiments. SB and RD were involved in the preparation and purification of protein. SP, BM, and SS helped HP in the analysis of the results. GM synthesized





and characterized all the coumarin derivatives. NS and UCH were performed theoretical work and prepared the manuscript with the help of other authors. UCH designed and supervised the work.

## Conflicts of interest

The authors declare no competing financial interest.

## Acknowledgements

Financial support of University Grants Commission UGC-CAS-II and DST-PURSE-II (Govt. of India) Program of Department of Chemistry, Jadavpur University, Kolkata are greatly acknowledged. The authors also wish to acknowledge the financial support received from Dr D. S. Kothari Fellowship of Dr Barun Mandal.

## Notes and references

- 1 R. N. Rambaran and L. C. Serpell, *Prion*, 2008, **2**, 112–117.
- 2 M. B. Pepys, *Philos. Trans. R. Soc., B*, 2001, **356**, 203–211.
- 3 J. He, *Protein Sci.*, 2006, **15**, 213–222.
- 4 V. Villegas, J. Zurdo, V. V. Filimonov, F. X. Avilés, C. M. Dobson and L. Serrano, *Protein Sci.*, 2000, **9**, 1700–1708.
- 5 J. W. Kelly, *Curr. Opin. Struct. Biol.*, 1996, **6**, 11–17.
- 6 J. W. Kelly, *Structure*, 1997, **5**, 595–600.
- 7 J. W. Kelly, *Proc. Natl. Acad. Sci. U. S. A.*, 1998, **95**, 930–932.
- 8 J. C. Sacchettini and J. W. Kelly, *Nat. Rev. Drug Discovery*, 2002, **1**, 267–275.
- 9 *Dye Lasers*, ed. F. P. Schäfer, Springer Berlin Heidelberg, Berlin, Heidelberg, 1973, vol. 1.
- 10 N. Farinola and N. Piller, *Lymphatic Res. Biol.*, 2005, **3**, 81–86.
- 11 F. J. Duarte, L. S. Liao, K. M. Vaeth and A. M. Miller, *J. Opt. A: Pure Appl. Opt.*, 2006, **8**, 172–174.
- 12 G. Kontopidis, C. Holt and L. Sawyer, *J. Dairy Sci.*, 2004, **87**, 785–796.
- 13 R. Aschaffenburg and J. Drewry, *Biochem. J.*, 1957, **65**, 273–277.
- 14 Z. Teng, R. Xu and Q. Wang, *RSC Adv.*, 2015, **5**, 35138–35154.
- 15 M. Kuruvilla and C. Gurk-Turner, *Baylor Univ. Med. Cent. Proc.*, 2001, **14**, 305–306.
- 16 E. Anderes, S. Nand, *Handbook of Clinical Neurology Part II*, 2014, vol. 120, pp. 1125–1139.
- 17 D. D. Soto-Ortega, B. P. Murphy, F. J. Gonzalez-Velasquez, K. A. Wilson, F. Xie, Q. Wang and M. A. Moss, *Bioorg. Med. Chem.*, 2011, **19**, 2596–2602.
- 18 M. Akbarian, E. Rezaie, F. Farjadian, Z. Bazayr, M. Hosseini-Sarvari, E. M. Ara, S. A. Mirhosseini and J. Amani, *RSC Adv.*, 2020, **10**, 38260–38274.
- 19 E. Quezada, F. Rodríguez-Enríquez, R. Laguna, E. Cutrín, F. Otero, E. Uriarte and D. Viña, *Molecules*, 2021, **26**, 4550.
- 20 U. Kayal, R. Karmakar, D. Banerjee and G. Maiti, *Tetrahedron*, 2014, **70**, 7016–7021.
- 21 N. Sepay, S. Mallik, C. Guha and A. K. Mallik, *RSC Adv.*, 2016, **6**, 96016–96024.
- 22 S. Maity, S. Pal, S. Sardar, N. Sepay, H. Parvej, J. Chakraborty and U. Chandra Halder, *RSC Adv.*, 2016, **6**, 112175–112183.
- 23 S. Sardar, M. Anas, S. Maity, S. Pal, H. Parvej, S. Begum, R. Dalui, N. Sepay and U. C. Halder, *Int. J. Biol. Macromol.*, 2019, **125**, 596–604.
- 24 M. Collini, L. D'Alfonso and G. Baldini, *Protein Sci.*, 2000, **9**, 1968–1974.
- 25 G. V. Semisotnov, N. A. Rodionova, O. I. Razgulyaev, V. N. Uversky, A. F. Gripas' and R. I. Gilmanshin, *Biopolymers*, 1991, **31**, 119–128.
- 26 C. Bhattacharjee, S. Saha, A. Biswas, M. Kundu, L. Ghosh and K. P. Das, *Protein J.*, 2005, **24**, 27–35.
- 27 S. Maity, S. Pal, S. Sardar, N. Sepay, H. Parvej, S. Begum, R. Dalui, N. Das, A. Pradhan and U. C. Halder, *New J. Chem.*, 2018, **42**, 19260–19271.
- 28 M. Nilsson, *Methods*, 2004, **34**, 151–160.
- 29 W. W. Yu, E. Chang, J. C. Falkner, J. Zhang, A. M. Al-Somali, C. M. Sayes, J. Johns, R. Drezek and V. L. Colvin, *J. Am. Chem. Soc.*, 2007, **129**, 2871–2879.

